Scientific paper

Mechanical Performance and Durability of Latex-Modified Fiber-Reinforced Concrete

Gia Toai Truong[1], Min-Kyoung Son[2] and Kyoung-Kyu Choi[3*]

Received 9 July 2018, accepted 28 January 2019 doi:10.3151/jact.17.79

Abstract
In this study, the mechanical performance and durability of latex-modified fiber-reinforced concrete were experimentally investigated. For these purposes, various types of tests were carried out: compressive, flexural, restrained drying shrinkage, water-tightness, and freeze and thaw tests. In total, 59 test specimens were manufactured and performed in this study. The latex weight fractions of 10, 15, and 20% and the fiber volume fractions of 0.2 and 0.3% were used as main test parameters. For each fiber volume fraction, amorphous and conventional steel fibers having the same amount were used together. Based on the test results, it was found that the use of 15% latex weight fraction could result in the very early development of concrete compressive strength at the seventh day; the ratio between the concrete compressive strengths at the seventh and 28th days was approximately 91%. The use of a 0.3% fiber volume fraction presented a higher concrete compressive strength at the seventh day than that of a 0.2% fiber volume fraction. In addition, the increase of the latex weight fraction up to 20% increased the flexural strength, and the increase of the fiber volume fraction up to 0.3% also increased the flexural strength. Moreover, using a high amount of latex could delay the crack development time while the final crack width was almost the same. The addition of latex and fibers into the concrete matrix also resulted in excellent resistances of permeability and freeze-thaw cycles.

1. Introduction
Concrete materials are widely used in various structures including buildings, infrastructures, and pavement. Nevertheless, concrete materials still have many disadvantages, including low tensile strength, high porosity, and low resistance to freeze-thaw, chloride, and other environmental conditions (Popovics 1992). Thus, concrete structures could undergo deterioration under a service load, in particular, when subjected to harsh weather conditions. For example, pavement concrete could be cracked or broken as time progresses due to vehicle load, and drying shrinkage with the soil beneath the pavement concrete layer was considered as restraint. In addition, the use of deicing salts for melting snow resulted in the penetration of chloride ion into the concrete, and the drying and wetting cycles could lead to fast degradation of the concrete structures (Green *et al.* 2000). In order to overcome such weaknesses, polymer-modified concretes (e.g., latex, water soluble, epoxy resin, powdered emulsion) have recently come to be widely used in concrete structures (Bedi *et al.* 2013; Kuhlmann 1985; Nabavi *et al.* 2013).

According to the study by Ariffin *et al*. (2018), the addition of latex into the concrete matrix could significantly reduce the void ratio and increase the compressive strength of concrete. Ariffin *et al*. (2018) showed that the use of 5% liquid latex polymer increased the concrete compressive strength up to 133.3%. Ion *et al*. (2013) investigated whether the use of epoxy resin could result in a higher influence on the workability of the resulting concrete than the use of other types. The slump of concrete matrix having 10% epoxy resin was about 67 mm whereas those of concrete matrices having 10% polyurethane and 0.6% methylcellulose were 7 and 58 mm, respectively. In comparison with normal concrete, polymer-modified concrete also exhibited enhanced durability due to the formation of polymer film and the filling of capillary pores caused by polymer particles that could prevent the penetration of moisture and chloride ions (Wang *et al*. 2006; Wang *et al*. 2015). For all of these reasons, from literature reviews conducted by previous studies (Lee and Kim 2018; Abdel-Mohti *et al*. 2018; Oh *et al*. 2014; Muhammad and Ismail 2012; Lee *et al*. 2017; Li *et al*. 2010), it was found that the mechanical properties and durability of polymer-modified concrete still need further investigations for further applications.

Lee and Kim (2018) investigated the effects of shrinkage reducing agent (SRA) on the durability performance of the latex-modified concrete. The use of higher amounts of SRA showed a higher reduction of the drying shrinkage strain of the concrete and resulted in a greater penetration resistance of the chloride ions. Li *et al*. (2010) studied the influences of steel fibers on the mechanical properties of styrene-butadiene-rubber (SBR) latex-modified concrete. The test results showed that the addition of steel fibers into latex-modified con-

[1]PhD Student, School of Architecture, Soongsil Univ., 369 Sangdo-ro, Dongjak-gu, Seoul (06978), South Korea.
[2]Master Student, School of Architecture, Soongsil Univ., 369 Sangdo-ro, Dongjak-gu, Seoul (06978), South Korea.
[3]Associate Professor, School of Architecture, Soongsil Univ., 369 Sangdo-ro, Dongjak-gu, Seoul (06978), South Korea. *Corresponding author,
E-mail: kkchoi@ssu.ac.kr

Table 1 Geometric and material properties of fibers.

Fiber types	Length (mm)	Fiber thickness or diameter (μm)	Tensile strength (MPa)	Aspect ratio (L/D)	Specific mass (kg/m^3)	Shape
Amorphous metallic fiber	15	24[(1)]	1,600	625	7,200	Straight
Conventional steel fiber	13	200[(2)]	2,650	65	7,850	Straight

[(1)] Fiber thickness
[(2)] Fiber diameter

crete matrix could significantly improve the flexural and compressive strength. Such increases were a function of fiber dosage. In addition, Xu *et al*. (2014) also found that the flexural toughness and impact toughness of SBR latex-modified concrete increased significantly as a result of the addition of the polyester fibers into the matrix. However, such mechanical properties of latex-modified fiber-reinforced concrete differ with different fiber types (Kim and Park 2013). In a sulfated environment, the use of natural rubber latex (NRL) helped to effectively resist the strength loss of the concrete matrix due to the appearance of latex particles in the capillaries and voids. On the contrary, in an acidic environment, the natural rubber latex-modified concrete showed lower compressive strength than that of the normal concrete. The use of more NRL led to a lower concrete compressive strength (Muhammad and Ismail 2012).

In the previous studies by Choi and Ku (2015b) and Choi *et al*. (2015a, 2015c), amorphous metallic (AMF) and conventional steel fibers (CSF) were used to investigate their effects on the material characteristics of concrete. The test results showed that both AMFs and CSFs could delay the crack development time, reduce the drying shrinkage strain, and improve the flexural and shear behaviors of concrete. However, the AMFs were more effective in controlling the material characteristics of concrete than the CSFs. In the present study, the hybrid fibers composed of amorphous metallic and conventional steel fibers were used to evaluate the mechanical performance and durability of latex-modified fiber-reinforced concrete through the experimental program including compressive, flexural, restrained drying shrinkage, water-tightness, and freeze and thaw tests. The latex weight fractions used were 10, 15, and 20%, respectively; and the hybrid fiber volume fractions used were 0.2 and 0.3%, respectively. Based on the various types of tests, the material characteristics of latex-modified fiber-reinforced concrete were investigated.

2. Experimental program
2.1 Materials

In this study, Styrene-Butadiene latex (or simply latex) composed of two main hydrocarbon monomers of styrene and butadiene was used as a modified material for concrete. The latex used is a milky liquid material and has a solid content of 48.5%, a viscosity of 130 cps, and a pH of 9.5. The advantages of this latex were its abilities to increase resistances to rutting and shoving, low temperature cracking, and load-associated fatigue cracking, and also to reduce temperature susceptibility (Wang *et al*. 2015).

Two types of fibers were employed in this study: conventional steel fibers (CSF) and amorphous metallic fibers (AMF). **Table 1** presents the geometrical and material properties of the fibers used in this study. As shown in **Table 1**, the conventional steel fibers (CSF) used have a straight shape with a length of 13 mm and a diameter of 200 μm. Thus, the aspect ratio of CSF, which was defined to be the ratio between the length and the diameter, was approximately 65. The amorphous metallic fibers (AMF) used were made of an amorphous alloy of the Fe family with a specific mass of 7,200 kg/m^3. The AMFs used also had a straight shape with a length of 15 mm and a thickness of 24 μm. Therefore, the aspect ratio of AMF was much higher than that of CSF with a value of 625. According to Choi *et al*. (2015a), the extremely thin thickness of the amorphous metallic fibers allows for their excellent dispersion in concrete mixing. Thus, the workability of the fiber reinforced concrete can be significantly improved.

Figure 1 presents the scanning electron microscopy (SEM) photos of the amorphous metallic (AMF) having a thickness of 24 μm and the conventional steel fibers (CSF) having a thickness of 200 μm. As shown in **Fig.**

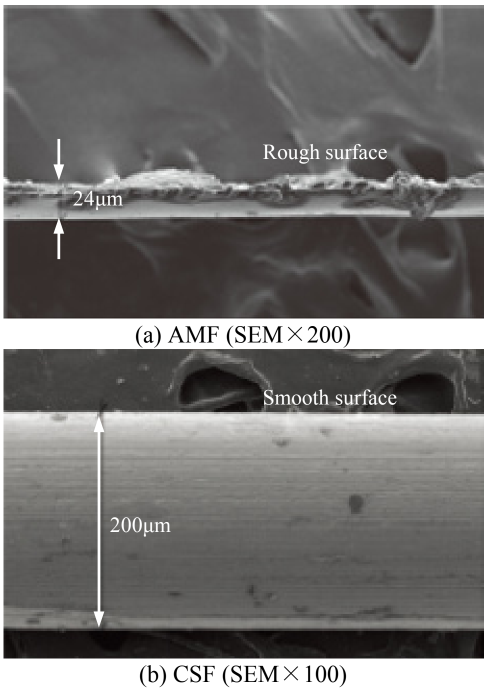

(a) AMF (SEM×200)

(b) CSF (SEM×100)

Fig. 1 Scanning electron microscopy (SEM) photos of amorphous metallic (AMF) and conventional steel fibers (CSF).

Table 2 Concrete mix proportions.

Batch	Slump (mm)	Air condition (%)	W/C	S/a(1) (%)	Unit content (kg/m^3)						Admixture (%)
					Latex	Water	Cement	Fine aggregate	Coarse aggregate	Fiber	
L10-F0.3	160	5.3	0.47	58	49.5	207	494.5	795	586.6	23.4 (11.7(2))	0.4
L15-F0.2	150	6.0	0.47	50.7	74.2	191.7	494.5	767.4	745.5	15.6 (7.8)	0.2
L15-F0.3	165	6.2	0.45	50.7	74.2	185.6	494.5	787.4	764.9	23.4 (11.7)	0.2
L20-F0.3	165	6.1	0.42	50.7	98.9	157	494.5	696.5	689.7	23.4 (11.7)	0.2

(1) S/a = sand to aggregate ratio
(2) The weight of amorphous metallic fibers

1a, the surface of the amorphous metallic fiber was rather rough, which was expected to enhance the bond strength between the fibers and the cementitious materials (Choi *et al*. 2015a). In contrast, the surface of the conventional steel fiber was relatively smooth (**Fig. 1b**). Despite the fact that the amorphous metallic and conventional steel fibers showed different geometrical and mechanical behaviors, a combination of these two fiber types was applied in this study in order to investigate the effect of hybrid fibers on the mechanical properties of latex-modified concrete. In this study, the hybrid fiber volume fractions (or fiber volume fractions) used were 0.2 and 0.3%. For each fiber volume fraction, the amount of amorphous and conventional steel fibers was the same.

A conventional Portland cement with a specific mass of 3,150 kg/m^3 and a Blaine fineness of 320 m^2/kg was used in this study. Stones with a maximum size of 20 mm and surface dried specific gravity of 2,690 kg/m^3 were used as coarse aggregates, and natural sand with a surface dried specific gravity of 2,600 kg/m^3 and fineness modulus of 2.6 were used as fine aggregates.

2.2 Mix proportions

Table 2 presents the various mix proportions of concrete used in this study. In **Table 2**, the batch name indicates the addition of latex and fiber contents into the concrete mix proportion. For example, batch L10-F0.3 means that a latex weight fraction of 10% and a fiber volume fraction of 0.3% were added into the concrete mixture. The mix proportions were intentionally designed to acquire nearly identical slumps and air conditions for all batches. From the test results, the slumps obtained were almost the same with values ranging from 150 to 165 mm, while the air condition was in a range of 5.3-6.2% (**Table 2**). The design compressive strength of concrete was 21 MPa for concrete batches L10-F0.3, L15-F0.2, and L15-F0.3, and 24 MPa for concrete batch L20-F0.3 after 28 days.

For that purpose, the mix proportion of each concrete batch was determined. As shown in **Table 2**, the ratio between water and cement ranged from 0.42 to 0.47; the ratio between sand and total aggregate ranged from 50.7 to 58%; the unit content of latex ranged from 49.5 to 98.9 kg/m^3, which corresponds to weight fractions of 10, 15, and 20% and fiber volume fractions of 0.2 and 0.3%.

The manufacturing procedure of the concrete batches is as follows: First, natural sand, stone, and cement were dry-mixed for approximately two minutes. Then, the water containing hybrid fibers and latex was gradually added to the mixture according to the water-to-cement ratio, fiber volume fraction, and latex weight fraction mentioned in **Table 2**. The mixture continued to be wet-mixed for approximately four minutes, so as to ensure the fibers were uniformly dispersed in the mixture. Then, the concrete mixture was immediately cast into molds to make test specimens with configurations as requirements for concrete compressive, flexural, restrained drying shrinkage, water-tightness, and freeze-thaw resistance tests. All of the test specimens were then wrapped in plastic sheets for two days in order to prevent moisture loss.

2.3 Concrete compressive test

The compressive strength of concrete was tested according to test standard KS F 2405 (KS 2010) using a universal testing machine (UTM) having a loading capacity up to 1000 kN. The test specimens were in a cylinder shape with a dimension of 100 × 200 mm (diameter × height). After two days, all test specimens were removed from wrapping (as described in section 2.2) and cured at room temperature (approximately 11°C) with a relative humidity of 95%. The compressive strength of concrete was measured at the seventh and 28th days. The test parameters were the latex weight fraction (0, 10, 15, and 20%) and hybrid fiber volume fraction (0, 0.2, and 0.3%). In total, four test series were cast and tested including C-L10-F0.3, C-L15-F0.2, C-L15-F0.3, and C-L20-F0.3, where "C" indicates the compressive test of concrete. For each test series, at each testing time, three replicas of the test specimens were examined.

2.4 Flexural test

Figure 2 shows the flexural test apparatus. This four-point bending test was performed in accordance with KS F 2408 (KS 2016) with a loading rate of 0.05 mm/min. The test specimens were prismatic beams with dimensions of 100 × 100 × 400 mm (width × height × length, see **Fig. 2a**). All test specimens were demolded on the second day of concrete aging after casting and curved at room temperature (approximately 11°C) with a relative humidity of 95%. The flexural tests were performed on the 28th day of concrete aging. In this study, four test series were carried out: F-L10-

F0.3, F-L15-F0.2, F-L15-F0.3, and F-L20-F0.3, where “F” indicates the flexural test of concrete. For each test series, three replicas of the test specimens were cast. The test was intentionally terminated when the applied load reached 30% of the peak load in the descending branch. According to KS F 2408 (KS 2016), the flexural strength (f_b) can be calculated as

$$f_b = \frac{PL}{bh^2} \tag{1}$$

where L is the shear span (= 100 mm), b and h are the width and height of the beams ($b = h = 100$ mm), and P is the applied load (kN).

2.5 Restrained drying shrinkage test

In this study, ring restrained drying shrinkage tests were carried out according to the test standard ASTM C1581-04 (ASTM 2004) in order to investigate the cracking behavior of the concrete caused by restrained shrinkage. **Figure 3** presents the dimensions and test setup of the ring test specimens. After curing for two days, the outer steel molds of the ring test specimens were removed. The bottom and top surfaces of the concrete ring specimens were sealed with a steel base and silicon rubber, respectively. This condition was to allow for the concrete ring specimens to dry from the outer circumferential surface, and to ensure that shrinkage would be uniform through the height of the specimen.

The restrained shrinkage tests were carried out under the laboratory condition of a temperature of 11 ± 2°C and a relative humidity of 55 ± 10%. Two test series of R-L15-F0.3 and R-L20-F0.3 with three replicas of test specimens for each test series investigated, where “R” indicates the ring test of the concrete. Two steel strain gauges were attached to an inner steel ring in order to measure the strain of the steel ring (see **Fig. 3**). The

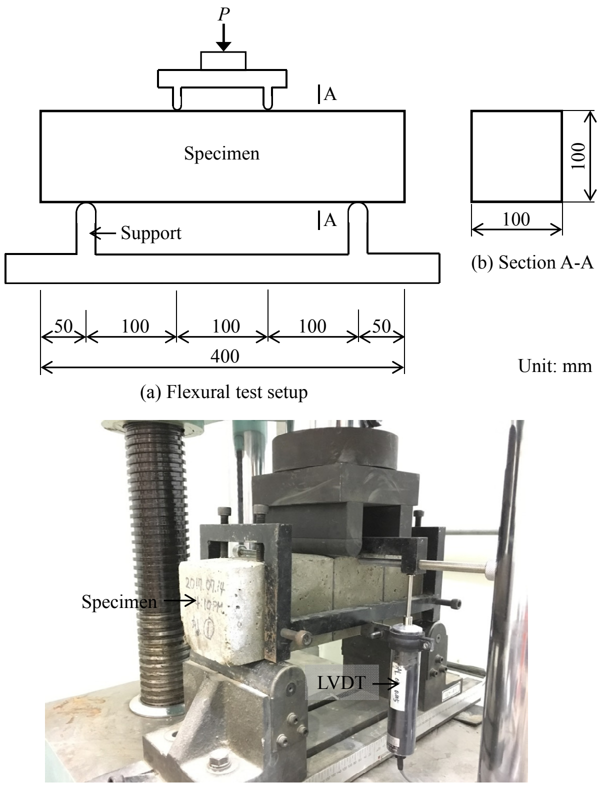

Fig. 2 Flexural test apparatus.

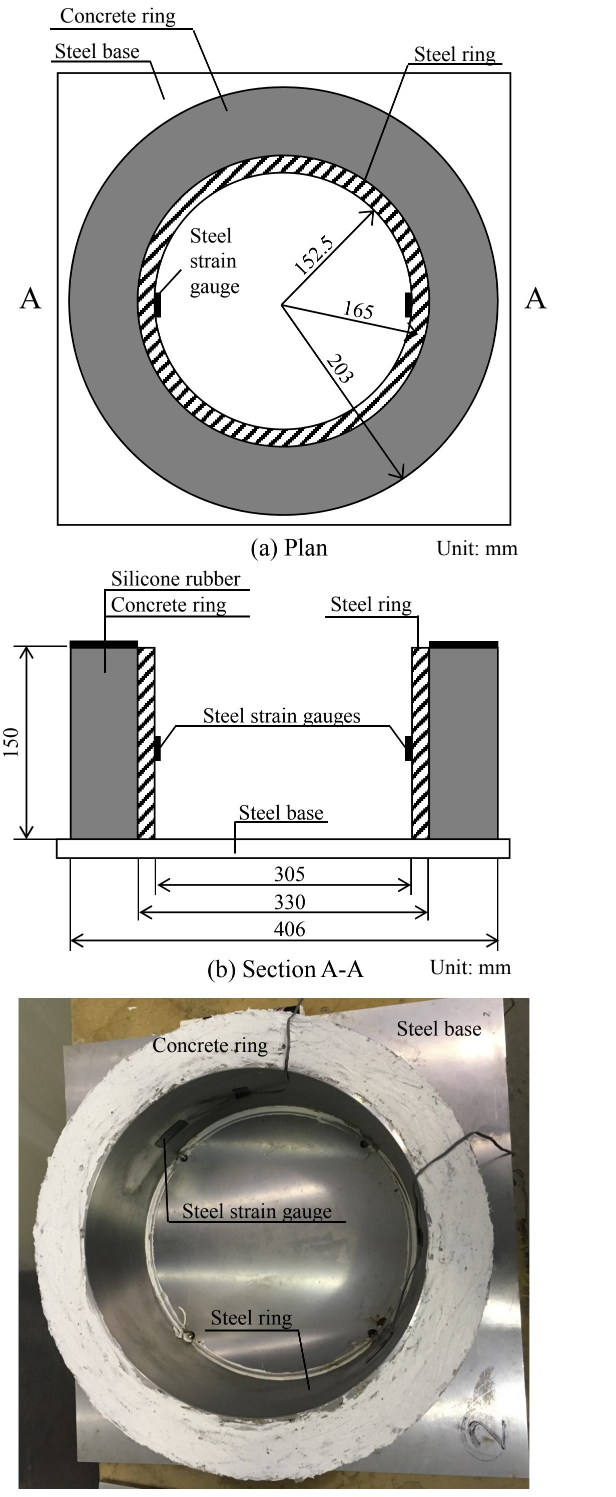

Fig. 3 Geometry of ring specimens.

steel strain, temperature, and humidity were acquired using a data logger system. The test data were taken every 15 minutes. A microscope with a resolution of 0.01mm was used to measure the crack width of the test specimens. The crack width measurement was taken every day. In this study, the crack width presented was the average value of three test specimens in each series.

2.6 Water-tightness test

The water-tightness test in this study was performed in accordance with the guidance specified in KS F 2609 (KS 2008b) in order to investigate the tightness (relative to water) of the latex-modified hybrid fiber-reinforced concrete. The water-tightness test system is presented in **Fig. 4**. The test specimen has a length of 100 mm, a width of 50 mm, and a height of 30 mm. On the second day of concrete aging after casting, all test specimens were demolded and then cured at room temperature (approximately 20°C) with a relative humidity of 65 ± 5%. On the 28th day of concrete aging, all of the test specimens were dried to a constant weight, and two end surfaces were coated with epoxy. This was to allow the water absorption to proceed along the length of the test specimen. Then, the test specimens were immersed in water to a depth of 5 mm. The water absorption capacity (ω) of the test specimens was measured at various durations, including 10 mins, 30 mins, 1 hour, 6 hours, and 24 hours, according to KS F 2609 (KS 2008b).

$$\omega = m / \sqrt{t} \tag{2}$$

where m (kg/m^2) is the weight of water absorbed after a duration t (h).

In this study, three test series were fabricated and tested: W-L15-F0.2, W-L15-F0.3, and W-L20-F0.3,

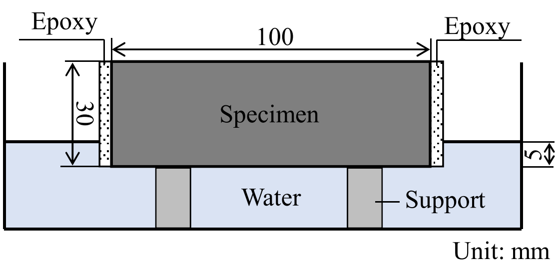

Fig. 4 Water-tightness test system.

where "W" indicates the water-tightness test. For each test series, four replicas of each test specimen were cast.

2.7 Freeze-thaw resistance test

The freeze-thaw resistance test was carried out according to KS F 2456 (KS 2008a) in order to examine the durability of the latex-modified hybrid fiber-reinforced concrete. In this test, the specimens were exposed to a freeze-thaw cycle in an appropriate chamber with temperatures ranging from -18 to 4°C. Each test specimen was subjected to 300 freeze-thaw cycles, and each cycle of freezing and thawing lasted four hours. **Figure 5** shows the freeze-thaw resistance test apparatus. The durability of the test specimen was characterized by the relative dynamic modulus of elasticity (P_c) after the c-th cycle of freezing and thawing, which was calculated according to KS F 2456 (KS 2008a).

$$P_c = \left(\frac{n_c}{n_0} \right)^2 \times 100 \tag{3}$$

where n_c is the fundamental transverse frequency after the c-th cycle of freezing and thawing, and n_0 is the initial fundamental transverse frequency.

In this study, one test series FT-L15-F0.3 with five replicas of the test specimen were cast and tested, where "FT" indicates the freeze-thaw resistance test. The test specimens were in prismatic shape with the dimensions of 100 × 100 × 400 mm (width × height × length).

3. Test results and discussion

3.1 Concrete compressive strength

The compressive strengths of the latex-modified fiber-reinforced concretes are presented in **Fig. 6** and **Table 3**. Note that for each test series, at each testing time, three replicas of the test specimens were investigated. As shown in **Table 3**, the obtained test results showed a fluctuation even though three duplicates were cast in the same batch. Thus, in this study, the medium value neglecting the lowest and highest ones was used as well as the average values. In general, the medium values exhibited the same trend as the average values. The development of concrete compressive strength at an early age plays an important role during construction work and shortens the form removal time, which could reduce the

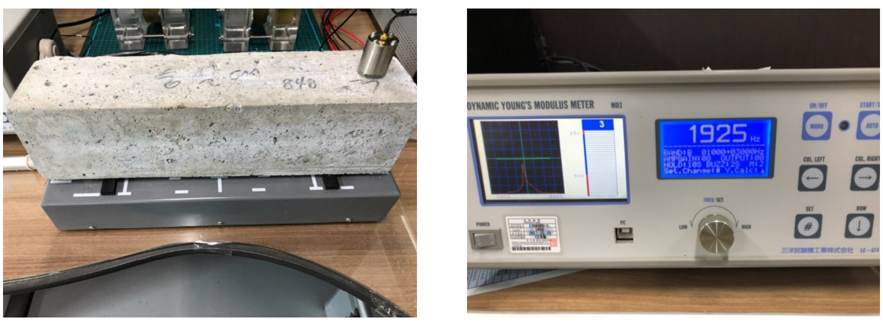

(a) Test specimen (b) Transverse frequency apparatus

Fig. 5 Freeze-thaw resistance test apparatus.

Table 3 Compressive strength of latex modified fiber reinforced concrete.

Test specimens	Compressive strength (MPa)			
	7th day	Average (medium) at 7th day	28th day	Average (medium) at 28th day
C-L10-F0.3	17.18	17.52 (17.18)	22.99	22.64 (22.99)
	20.14		25.82	
	15.25		19.1	
C-L15-F0.2	11.35	13.00 (12.18)	18.15	17.65 (17.73)
	14.87		17.73	
	12.18		17.07	
C-L15-F0.3	19.41	20.85 (19.41)	24.78	22.98 (23.64)
	17.63		23.64	
	25.50		20.52	
C-L20-F0.3	16.85	21.01 (23.03)	28.15	25.81 (26.68)
	23.03		22.6	
	23.13		26.68	

construction period as well as costs (Yoon *et al*. 2017). **Figure 6a** presents the effects of different amounts of latex on the early-age compressive strength of concrete. The figure shows that the use of a higher amount of latex could result in a greater compressive strength of concrete at an early age. In the case of specimen C-L10-F0.3 using a latex weight fraction of 10%, the average compressive strength at the seventh day ($f'_{c,7}$) was 17.52 MPa; meanwhile those of specimens C-L15-F0.3 and C-L20-F0.3 using the latex weight fractions of 15 and 20% were 20.85 and 21.01 MPa, respectively (see **Table 3**). However, since the concrete compressive strengths obtained from the test results at the 28th day (f'_c) were different, the concrete strength at the seventh day was normalized by the concrete compressive strength at the 28th day, as shown in **Fig. 7**. In **Fig. 7a**, it is confirmed that the use of a high amount of latex could increase the concrete strength at an early age. The $f'_{c,7} / f'_c$ ratios were approximately 77, 91, and 81% for specimens C-L10-F0.3, C-L15-F0.3, and C-L20-F0.3 using latex weight fractions of 10, 15, and 20%, respectively. It could clearly be seen that by increasing the latex weight fraction up to 15%, the compressive strength of C-L15-F0.3 at the seventh day had already attained almost all of its compressive strength at 28th day. Meanwhile, the addition of 20% latex weight fraction showed a relatively low $f'_{c,7} / f'_c$ ratio compared to that of C-L15-F0.3. This is because when the dosage of latex reaches 20%, the surfaces of cement and aggregate particles would be covered by a dense polymer membrane, which disturbs the development of the hydration products such as calcium silicate hydrates (CSH) and ettringite (Xiao *et al*. 2017; Topcu and Atesin 2016). This could slightly delay the cement hydration process, and thus results in weak strength of concrete at the early age. Note that CSH appears in the form of a coating product around aggregate particles, and ettringite is

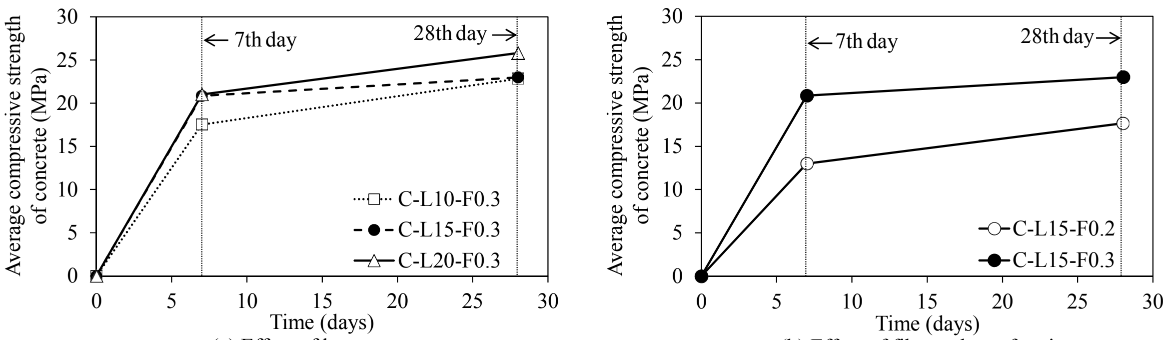

(a) Effect of latex amount (b) Effect of fiber volume fraction

Fig. 6 Compressive strength of latex modified fiber reinforced concrete at 7th and 28th day.

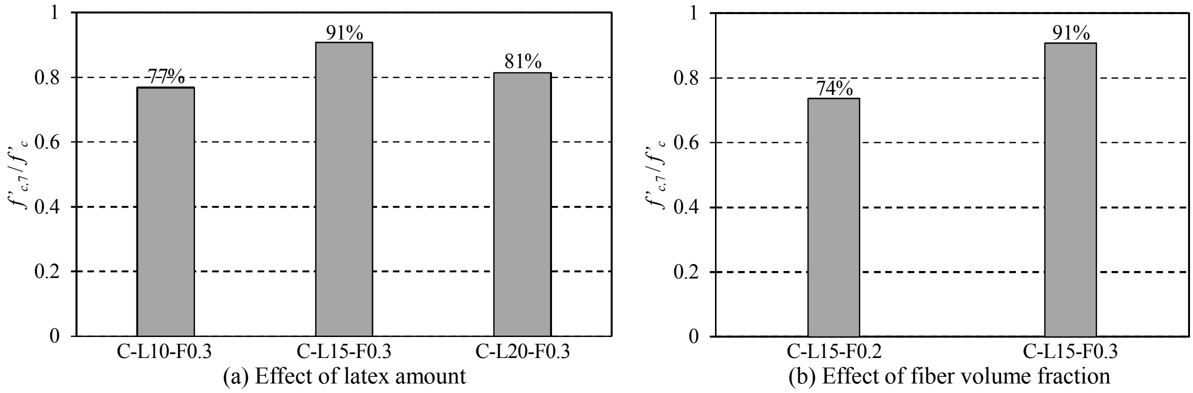

(a) Effect of latex amount (b) Effect of fiber volume fraction

Note: f'_c is the compressive strength of concrete at 28th day that obtained from the test results

Fig. 7 Effects of latex amount and fiber volume fraction on early-age compressive strength of concrete.

elongated into a needle-like shape.

The effect of fiber volume fraction on the concrete compressive strength at an early age is presented in **Fig. 6b**, which shows that the addition of high fiber volume fraction could significantly increase the early-age compressive strength of concrete. The concrete strengths at the seventh day of C-L15-F0.2 and C-L15-F0.3 using 0.2 and 0.3% fiber volume fraction were 13.00 and 20.85 MPa, respectively (see **Table 3**). The normalized concrete strength also confirmed this behavior (see **Fig. 7b**). According to the studies by Chan and Li (1997) and Hamad (2017), increasing the fiber volume fraction could result in an increase in the mechanical bond strength between fibers and matrix, where the use of fibers could delay the crack formation and arrest the crack propagation in the concrete specimens, and thus resulted in a higher compressive strength of concrete. In addition, such increase of compressive strength of concrete could also be attributed to the reduction in the porosity of fiber reinforced concrete owing to the use of fibers (Miloud 2005).

The compressive strengths of latex-modified fiber-reinforced concrete at the 28th day are also presented in **Table 3**; in the table, the concrete compressive strengths at the 28th day for specimens C-L10-F0.3, C-L15-F0.3, and C-L20-F0.3 were 22.64, 22.98, and 25.81 MPa, respectively, which were almost the same as the design compressive strength. Specimen C-L15-F0.2 showed a relatively lower compressive strength at the 28th day (17.65 MPa). However, in the cases of C-L10-F0.3 and C-L15-F0.3, the use of a high amount of latex could result in a higher concrete compressive strength at an early age, but those at the 28th day were almost the same. Meanwhile, the use of high fiber volume fraction showed a higher compressive strength of concrete at both the seventh and 28th days.

3.2 Flexural strength

Figure 8 shows the flexural strength versus the mid-span deflection relationships of test specimens in this study. The flexural strength (f_b) of the test specimens was determined at the point where the peak strength occurs, as defined in KS F 2408 (KS 2016). **Table 4** presents the flexural strengths of the test specimens in this study. In general, the use of a high amount of latex and a high fiber volume fraction significantly increased the flexural strength of concrete (see **Fig. 8** and **Table 4**). Regarding the effects of different amounts of latex (**Fig. 8a**), the average flexural strength of specimen F-L10-F0.3 using a latex weight fraction of 10% was 3.37 MPa (see **Table 4**). When increasing the latex amount up to 15 and 20%, the average flexural strength of specimens F-L15-F0.3 and F-L20-F0.3 increased up to 14.5 and 25.5%, respectively. This is because the presence of the superplasticizer agents on latex surfactants could help to increase the bond strengths between materials in the concrete matrix (Han *et al.* 2015). However, since the concrete compressive strength was different for each flexural test specimen, for easy comparison, the flexural strength was normalized by $\sqrt{f_c'}$ after Ramakrishnan *et al.* (1989), where f_c' (in MPa) is the compressive strength of concrete acquired from the test results. **Figure 9a** shows the normalized flexural strength ($f_b/\sqrt{f_c'}$) of the F-L10-F0.3, F-L15-F0.3, and F-L20-F0.3 specimens investigated in this study. In **Fig. 9a**, it is obvious that the addition of a high amount of latex

Table 4 Flexural test results.

Test specimens	Initial stiffness (kN/mm)	Average Initial stiffness (kN/mm)	Flexural strength, f_b (MPa)	Average flexural strength, f_b (MPa)
F-L10-F0.3	709.6	874.7	3.18	3.37
	1095.3		3.27	
	819.1		3.67	
F-L15-F0.2	611.2	521.3	2.67	2.95
	431.4		3.18	
	-(1)		2.99	
F-L15-F0.3	493.1	544.3	3.20	3.86
	633.8		4.25	
	506.0		4.13	
F-L20-F0.3	561.7	388.4	4.64	4.23
	330.1		4.06	
	446.7		3.98	

(1) Data missing

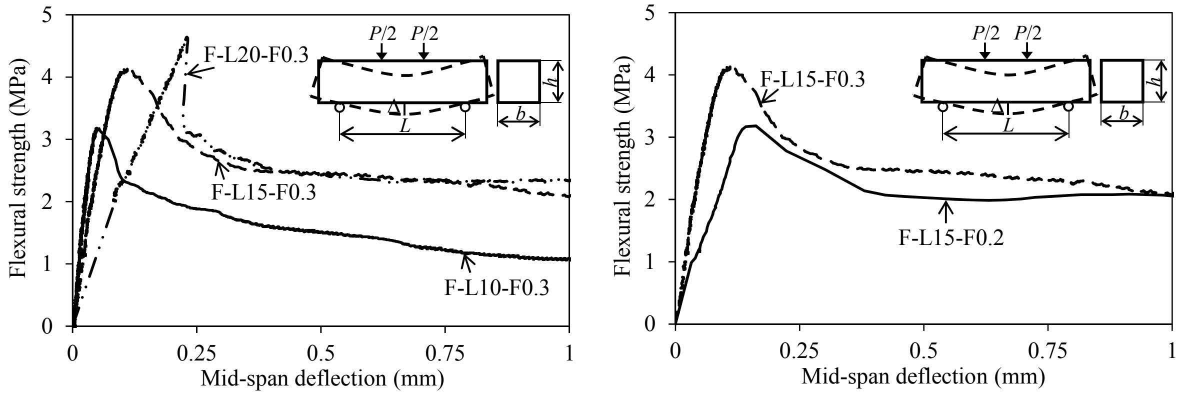

(a) Effect of latex amount (b) Effect of fiber volume fraction

Fig. 8 Flexural strength of latex modified fiber reinforced concrete.

significantly increased the flexural strength. The normalized flexural strength of F-L10-F0.3 using 10% latex weight fraction was 0.71; those of F-L15-F0.3 and F-L20-F0.3 using 15 and 20% latex weight fraction were 0.81 and 0.83, respectively. After reaching the peak strength, all test specimens showed an apparent decrease of strength in the descending branch. At the net deflection of $L/300$ (= 1 mm), the ratios between the residual strength and the flexural strength of specimens F-L15-F0.3 and F-L20-F0.3 were almost the same, with values of 54.7 and 55.6%, respectively. That of specimen F-L10-F0.3, on the other hand, was lower, with a value of 32.6%. In contrast to the flexural strength, the initial stiffness of the test specimens exhibited a trend toward decreasing as the amount of latex increased (see **Fig. 8a**). Note that the initial stiffness of the flexural test specimens was defined at the point corresponding to 30% of the peak load in the ascending branch. As shown in **Table 4**, the average initial stiffness of F-L10-F0.3, F-L15-F0.3, and F-L20-F0.3 specimens was 874.7, 521.3, and 388.4 kN/mm, respectively. The same observation was also noted in the study conducted by Diab *et al*. (2013). According to Diab *et al*. (2013), the presence of latex membranes might effectively prevent the propagation of micro-cracks within the concrete specimens, and thus could result in the increase of matrix deformation. This is owing to the effect of polymeric performance of latex. Thus, the initial stiffness shows a tendency to decrease as the latex dosage increases.

The effects of different fiber volume fractions on the flexural behaviors of concrete are presented in **Fig. 8b** and **Table 4**; these show that increasing the fiber volume fraction from 0.2 to 0.3% increased the average flexural strength from 2.95 MPa for specimen F-L15-F0.2 to 3.86 MPa for specimen F-L15-F0.3 (see **Table 4**). This behavior was confirmed by using the normalized flexural strength for F-L15-F0.2 and F-L15-F0.3 specimens as presented in **Fig. 9b**. In the figure, the normalized flexural strength of specimen F-L15-F0.2 using 0.2% fiber volume fraction was 0.70, which was less than the 0.81 of specimen F-L15-F0.3 using 0.3% fiber volume fraction. In a study by Choi and Ku (2015b), the same behavior was also observed. This is attributed to the fibers potentially transferring tensile stress between the cracking surface. Assuming that the fibers were perfectly dispersed in the concrete matrix, adding a higher fiber volume fraction should cause a higher tensile strength (Choi and Ku 2015b). However, F-L15-F0.2 and F-L15-F0.3 specimens exhibited almost the same initial stiffness at early stage with the values of 521.3 and 544.3 kN/mm, respectively. This observation was in contrast to that of the test specimens using latex as the main parameter. In the descending branch, the residual strengths of specimens F-L15-F0.2 and F-L15-F0.3 were almost the same at the net deflection of 1 mm. This means that F-L15-F0.2 showed a lower reduction of flexural strength than that of F-L15-F0.3. The ratios between the residual strengths and the flexural strengths of specimens F-L15-F0.2 and F-L15-F0.3 were 71.2 and 54.4%, respectively.

3.3 Ring restrained shrinkage

Figure 10 presents the steel strain profile of ring test specimens R-L15-F0.3 and R-L20-F0.3; in the figure, the steel strain exhibited high fluctuation, which was attributed to the instability of the relative humidity applied to the test specimens. In the case of specimen R-L15-F0.3 with a latex weight fraction of 15% (**Fig. 10a**), the steel strain increases up to the 10th day of concrete aging. After that, a sudden drop of strain profile was observed, which was caused by the development of visible cracks in the concrete ring (Choi *et al*. 2015c). However, by using a microscope, the cracking time of specimen R-L15-F0.3 was relatively late at the 18th day of concrete aging. Meanwhile, in the case of specimen R-L20-F0.3 (**Fig. 10b**), the use of a high amount of latex (20%) could significantly delay the crack development time of the concrete. The crack development time of R-L20-F0.3 was the 19th day of concrete aging. The same observation was also confirmed using a microscope. This is because as the high amount of latex was added, more latex elements with greater interface bonding were filled into the micro-pore of the concrete, leading to a delayed crack development time (Soroushian and Tlili 1991). After cracking, the strain profiles of specimens R-L15-F0.3 and R-L20-F0.3 showed a gradual reduction, due to the appearance of fibers in the concrete matrix.

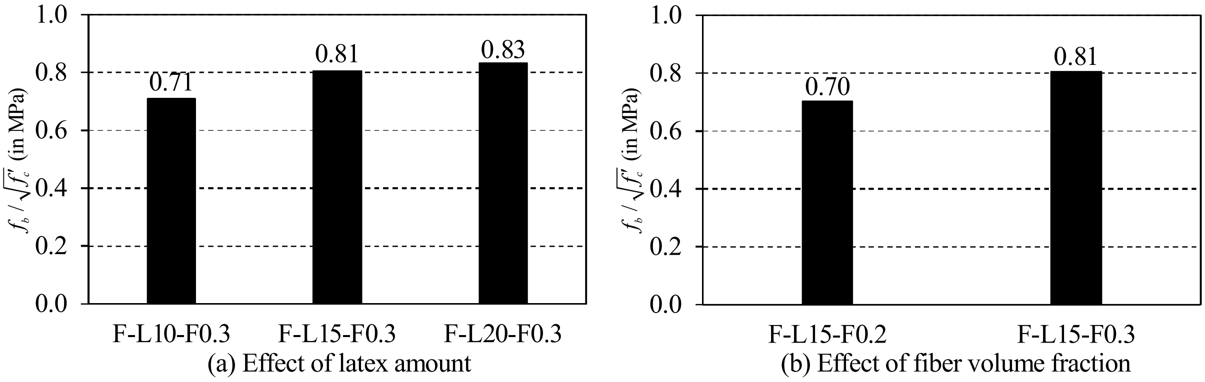

Fig. 9 Normalized flexural strength of the test specimens.

In this study, the previous model proposed by Choi *et al*. (2015) was adopted to predict the crack development time of ring test specimens. Such prediction model based on tensile stress and strength approach, as presented in Eq. (4).

$$\sigma_t \geq f_t \tag{4}$$

where, σ_t is the tensile stress developed due to concrete restraint, and f_t is the tensile strength of concrete.

The tensile stress of concrete as time development was determined as following:

$$\sigma_t(t) = E_c(t)\varepsilon_{sh}(t)\Omega(t) \tag{5}$$

$$\Omega(t) = \frac{E_s A_s}{E_c(t) A_c + E_s A_s} \leq 1 \tag{6}$$

where, $E_c(t)$ is the elastic modulus of concrete calculated according to ACI 318-14 (ACI 2014), $\Omega(t)$ is the degree of restraint of the concrete ring caused by steel ring, and $\varepsilon_{sh}(t)$ is the free dry shrinkage strain of concrete, which was predicted based on GL2000 model (2000). A_c and A_s are the cross sectional areas of the concrete and steel rings, respectively.

The tensile strength of concrete at age (t) was determined based on the guidance specified in CEB-FIP Model Code 1990 (CEB 1993), as follows:

$$f_t(t) = \lambda\left[f_{cm}(t)/10\right]^{2/3} \tag{7}$$

$$f_{cm}(t) = \beta_{cc}(t) f_c' \tag{8}$$

$$\beta_{cc}(t) = \exp\left[s\left(1-\sqrt{28/t}\right)\right] \tag{9}$$

where, λ is a strength parameter, s is a coefficient depending on the type of cement (s = 0.25 for Type I Portland cement), and f_c' is the 28th day compressive strength of concrete.

The crack development time of concrete ring test specimens is determined at the intersection point between tensile strength and stress curves as presented in **Fig. 11**. As shown in **Fig. 11**, crack development time of specimens R-L15-F0.3 and R-L20-F0.3 is 13 and 18 days, respectively, which is almost the same as that obtained from experimental results by strain profile.

Figure 12 presents the cracking development of the ring test specimens investigated in this study. In the figure, in general, at least two cracks have occurred in each test specimen. The increased number of cracks was expected to reduce the width of every single crack (Ahmed and Mishashi 2009). The average crack widths of ring test specimens in accordance with time are presented in **Fig. 13**, which shows that the initial crack width of specimen F-L20-F0.3 using a high amount of latex (20%) was much lower than that of specimen F-L15-F0.3 using a small amount of latex (15%). The ini-

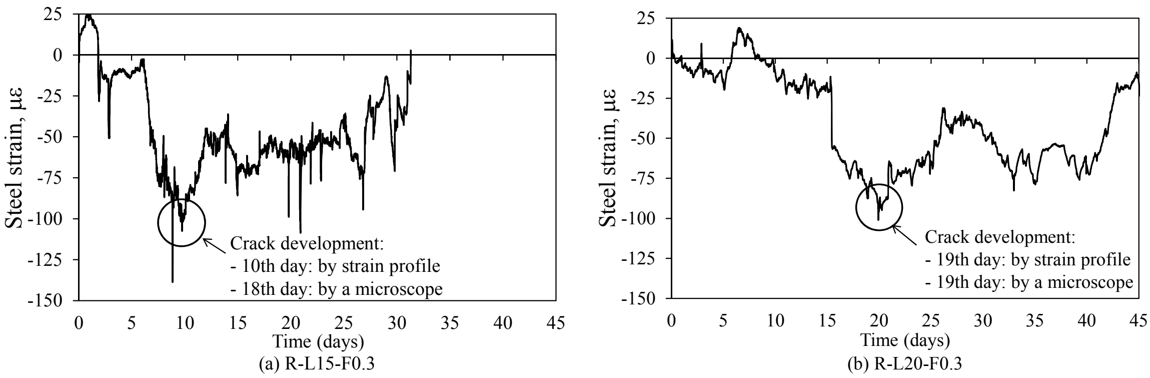

Fig. 10 Strain profile of ring test specimens.

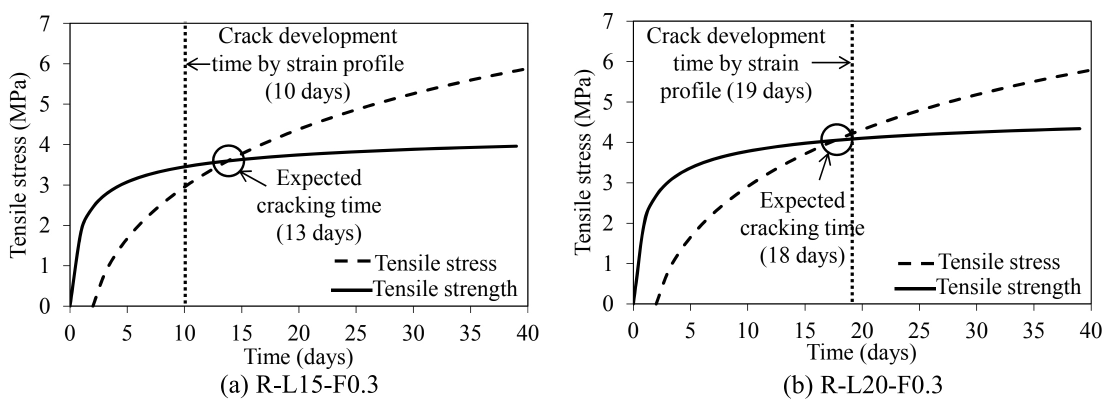

Fig. 11 Crack development time of ring test specimens by proposed model. (Choi *et al*. 2015a)

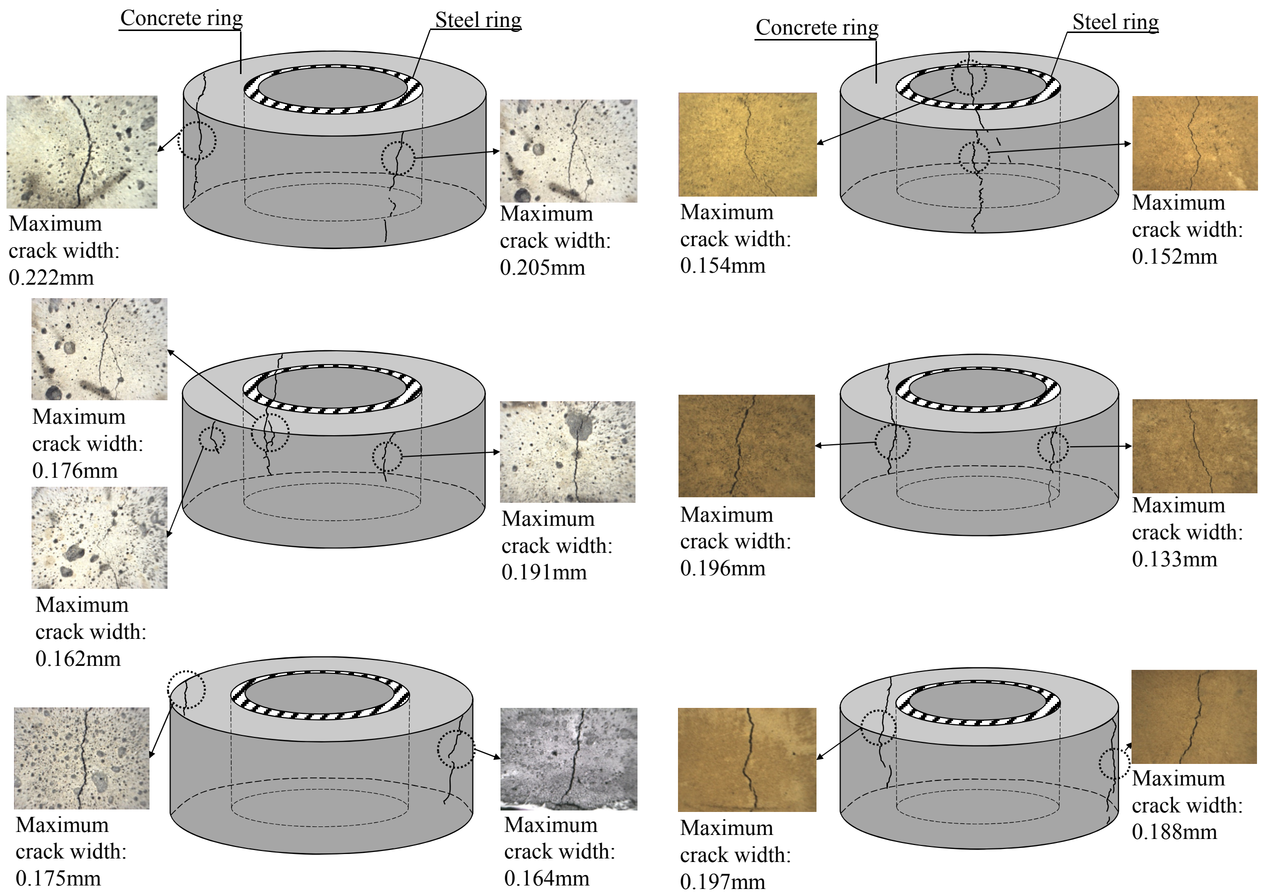

Fig. 12 Cracking development of ring test specimens.

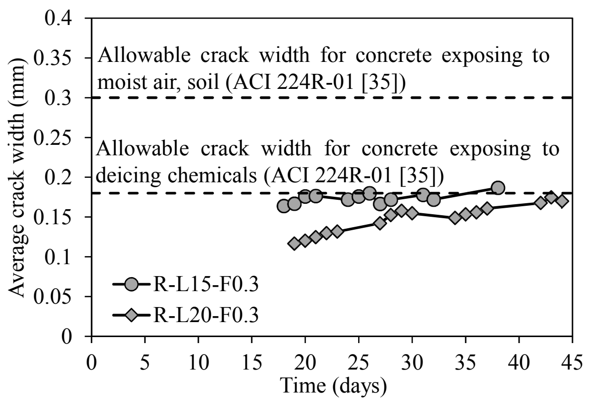

Fig. 13 Crack width of ring test specimens.

tial crack widths of F-L15-F0.3 and F-L20-F0.3 were 0.16 and 0.12 mm, respectively. As a concrete material, after initially cracking, the concrete drying causes the continuous widening of the crack width due to its quasi-brittle nature and low tensile strength (Diamaruya *et al.* 1997). Nevertheless, in this study, the addition of fibers and latex into concrete matrix significantly improved such brittle failure and enhanced the weak tensile behavior of concrete matrix (Han *et al.* 2015). Consequently, the test specimens F-L15-F0.3 and F-L20-F0.3 showed a very gradual increase of the crack width. The crack width of F-L15-F0.3 was 0.19 on the 38th day of concrete aging. This slightly exceeded the maximum allowable crack width of 0.18 mm for exposing concrete to the deicing chemicals specified in ACI 224R-0.1 (ACI 2001). However, this obtained crack width was much lower than the maximum allowable crack width of 0.3 mm for exposing concrete to moisture or soil (ACI 2001).

The same behavior was observed in the case of specimen F-L20-F0.3. However, due to the use of a high amount of latex, within the first 40 days, the crack width of F-L20-F0.3 was lower than that of F-L15-F0.3. Nevertheless, the final crack width of specimen F-L20-F0.3 (0.18 mm) was almost the same as that of F-L20-F0.3 (0.19 mm). In general, at the end of testing, the crack width of concrete was relatively small. This could explain the effectiveness of fibers and latex on transferring tensile stresses across the cracks, and thus results in capturing the crack widening. However, such observation was based on limited test data in this study, thus further research is needed for better understanding the drying shrinkage behavior of latex-modified fiber-reinforced concrete.

3.4 Water absorption capacity

The water absorption per area according to time of specimens W-L15-F0.2, W-L15-F0.3, and W-L20-F0.3

Table 5 Water-tightness test results of the test specimens in this study.

Specimens	Average weight of water absorption per area (kg/m^2)					Water absorption capacity, ω (kg/m^{2}h$^{0.5}$)	
	10 mins	30 mins	1 hour	6 hours	24 hours	For each specimen	Average
W-L15-F0.2	0.230	0.244	0.278	0.321	0.362	0.258	0.217
						0.210	
						0.228	
						0.173	
W-L15-F0.3	0.239	0.271	0.304	0.315	0.356	0.249	0.222
						0.228	
						0.212	
						0.199	
W-L20-F0.3	0.212	0.248	0.267	0.299	0.393	0.234	0.205
						0.163	
						0.223	
						0.199	

is presented in **Fig. 14** and **Table 5**; from the figure, it can be seen that the water absorption per area was almost the same for all test specimens. The use of various amounts of latex and fiber volume fractions did not considerably affect the permeability and absorption of the concrete in this study. In **Fig. 14**, the water absorption amount rapidly increased to approximately 0.267 to 0.304 kg/m^2 after being immersed in water for one hour. After that, the water absorption amount in the concrete specimens showed a relatively slow increase within 24 hours with a water absorption per area of approximately 0.356 to 0.393 kg/m^2 (see **Table 5**). This indicates that all specimens attained almost all of their saturation after just one hour.

From the water absorption per area obtained from the test results, the water absorption capacities (ω) of the test specimens were calculated, with the results presented in **Table 5**. In the table, the average water absorption capacities of the specimens W-L15-F0.2, W-L15-F0.3, and W-L20-F0.3 were 0.217, 0.222, and 0.205 kg/m^{2}h$^{0.5}$, respectively. These obtained values were much lower than the maximum acceptable value of 0.5 kg/m^{2}h$^{0.5}$ specified in KS F 4042 (KS 2012). Nevertheless, the use of higher latex amount or fiber volume fraction did not show considerable difference of water absorption capacity compared to that using low latex amount or fiber volume fraction. This is expected to be due to the combined effect of fibers and latex on the absorption capacity of latex-modified fiber-reinforced concrete. Further research is necessary to confirm this combined effect.

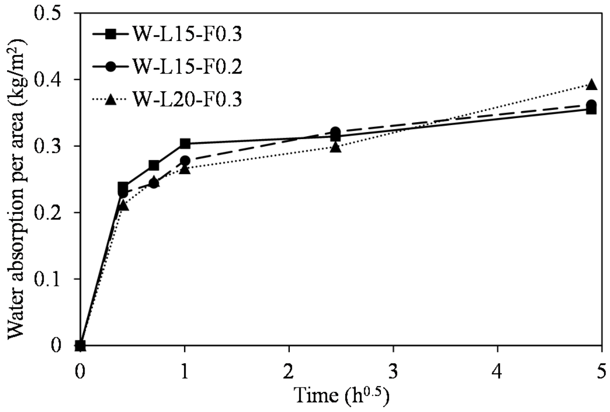

Fig. 14 Water absorption per area according to time.

3.5 Freeze and thaw

In this study, one test series with five test specimens (FT-L15-F0.3) was carried out. The relative dynamic modulus of elasticity (P_c) was calculated using Eq. (3). At the 300th cycle, the relative dynamic modulus of FT-L15-F0.3 ranged from 87.6 to 90.3% with a mean of 89.1% and a standard deviation of 1.27. The obtained test results were higher than the minimum requirement of 80% specified in the KS Concrete Structure Specification (MLIT 2009). This means that the latex-modified fiber-reinforced concrete could result in a good freeze and thaw resistance. Yang *et al*. (2018) also found that adding latex into the concrete mixture could significant improve the freeze and thaw resistance capacity of the concrete. In addition, such freeze and thaw resistance was increased with increasing the latex amount. This is because the presence of latex would provide better adhesion bonding between the aggregate and cement paste owing to the latex permeable membranes after cement hydration process, and thus resulted in a reduction of concrete deformation when subjected to freeze and thaw condition (Chandra *et al*. 1982).

4. Conclusions

In this study, the mechanical performance and durability of latex-modified fiber-reinforced concrete were investigated based on compressive strength, flexural strength, ring restrained shrinkage, water-tightness, and freeze and thaw tests. The main parameters used were the latex weight fraction (10, 15, and 20%) and fiber volume fraction (0.2 and 0.3%). The primary findings of the test results are as follows:

(1) The use of a high amount of latex and a high fiber volume fraction could increase the concrete compressive strength at an early age. In particular, the test specimen having 15% latex weight fraction (C-

L15-F0.3) exhibited very early strength development, showing an $f'_{c,7} / f'_c$ ratio of 91%. The test specimen having 0.3% fiber volume fraction showed 60.4% higher concrete compressive strength than that having 0.2% fiber volume fraction at the seventh day.

(2) The use of a high amount of latex amount and a high fiber volume fraction significantly affected the flexural strength and initial stiffness of concrete. Conspicuously, the use of 20% latex weight fraction increased the flexural strength up to 25.5% compared to the use of 10% latex weight fraction; but the initial stiffness of the test specimens decreased with the increase of latex amount. Meanwhile the use of 0.3% fiber volume fraction increased both the flexural strength and initial stiffness compared to the use of 0.2% fiber volume fraction.

(3) In ring test specimens, the use of high latex weight fraction could delay the cracking development time of the concrete. With 20% latex weight fraction, the crack development time was delayed from the 10th day to the 19th day compared to 15% latex weight fraction. The prediction model developed by Choi *et al*. (2015c) was adopted to predict the crack development time of latex-modified fiber-reinforced concrete. The prediction results by the Choi model were almost the same as the experimental results. Moreover, the addition of 20% latex weight fraction significantly reduced the crack width compared to the addition of 15% latex weight fraction. However, at the end of testing, the crack widths of R-L15-F0.3 and R-L20-F0.3 were almost the same.

(4) The test specimens in this study showed good permeability resistances with water absorption capacities ranging from 0.205 to 0.222, which were lower than the maximum acceptable value of 0.5 kg/m2h0.5 specified in KS F 4042. However, the use of various dosages of latex and fibers did not considerably affect the water absorption capacities of the concrete.

(5) The addition of latex and fibers into concrete could result in a good freeze and thaw resistance. In the case of specimen FT-L15-F0.3, the average relative dynamic modulus was 89.1%, which was higher than the minimum requirement of 80% specified in KS Concrete Structure Specification. However, the test data was limited, so further research is necessary to completely understand this behavior.

Acknowledgments

This work was supported by the National Research Foundation of Korea (NRF) grant funded by the Korea Government (Ministry of Education) (No. 2017R1D1A1B04033611).

References

Abdel-Mohti, A., Soliman, E. and Shen, H., (2018). "Thermal stability of latex modified mortars containing CNTs." *International Journal of Concrete Structures and Materials*, 12:40. Available at: <https://doi.org/10.1186/s40069-018-0265-4>

ACI, (2001). "*Control of cracking in concrete structures.*" ACI 224R-01, ACI Committee 224. American Concrete Institute, Farmington Hills, MI, USA.

ACI, (2014). "*Building code requirements for structure concrete*." ACI 318-14, ACI Committee 318, American Concrete Institute; Farmington Hills, Michigan, USA.

Ahmed, S. F. U. and Mihashi, H., (2009). "Restrained shrinkage-induced cracking of light weight high performance fiber reinforced cementitious composites." *American Journal of Engineering and Applied Sciences*, 2(4), 775-780.

Ariffin, N. F., Jaafar, M. F. Md., Lim, N. H. A. S., Bhutta, M. A. R. and Hussin, M. W., (2018). "Mechanical properties of polymer-modified porous concrete." *IOP Conf. Series: Materials Science and Engineering*, 342: 012081. Available at: <https://doi.org/10.1088/1757-899X/342/1/012081>.

ASTM, (2008). "*Standard test method for length change for length change of hardened hydraulic-cement mortar and concre*te." C157/157-08, ASTM International, West Conshohocken, PA, USA.

ASTM, (2004). "*Standard test method for determining age at cracking and induced tensile stress characteristics of mortar and concrete under restrained shrinkage*." ASTM C1581-04, ASTM International, West Conshohocken, PA, USA.

Bedi, R., Chandra, R. and Singh, S. P., (2013). "Mechanical properties of polymer concrete." *Journal of Composites*, 2013: Article 948745, 12 pages. Available at: <https://doi.org/10.1155/2013/948745>.

CEB (1993). "*CEB-FIP model code 1990.*" CEB Bulletin d'Information No 213/214, Comité Euro-International du Béton, Lausanne, Switzerland.

Chandra, S., Aavik, J. and Berntsson, L., (1982). "Influence of polymer microparticles on freeze-thaw resistance of structural lightweight aggregate concrete." *The International Journal of Cement Composites and Lightweight Concrete*, 4(2), 111-115.

Chan, Y-W. and Li, V. C., (1997). "Age effect on the characteristics of fiber/cement interfacial properties." *Journal of Materials Science*, 32, 5287-5292.

Choi, K-K., Choi, H. and Kim, J-C., (2015a). "Shrinkage cracking of amorphous metallic fibre-reinforced concrete." *Structures and Buildings*, 168(4), 287-297.

Choi, K-K. and Ku, D-O., (2015b). "Flexural behaviour of amorphous metal-fibre-reinforced concrete." *Structures and Buildings*, 168(1), 15-25.

Choi, K-K., Truong, G. T. and Choi, S-J., (2015c). "Restrained shrinkage cracking of amorphous metallic fibre-reinforced concrete." *Structures and Buildings*, 168(12), 902-914.

Choi, K-K., Truong, G. T., Kim, S-D. and Choi, I-R., (2015d). "Punching shear behaviour of shear reinforced concrete slabs." *Structures and Buildings*, 168(6), 402-420.

Diab, A. M., Elyamany, H. E. and Ali, A. H., (2013). "Experimental investigation of the effect of latex solid/water ratio on latex modified co-matrix mechanical properties." *Alexandra Engineering Journal*, 52, 83-98.

Diamaruya, M., Kobayashi, H. and Nonaka, T., (1997). "Impact tensile strength and fracture of concrete." *Journal de Physique IV Colloque*, 07(C3), C3-253-C3-258.

Gardner, N. J., (2000). "Design provisions for shrinkage and creep of concrete." In: A. Al-Manaseer, ed., *The Adam Neville Symposium: Creep and Shrinkage-Structural Design Effects*, SP-194, American Concrete Institute, Farmington Hills, MI, pp. 101-134.

Green, M. F., Bisby, L. A., Beaudoin, Y. and Labossiere, P., (2000). "Effect of freeze-thaw cycles on the bond durability between fibre reinforced polymer plate reinforcement and concrete." *Canadian Journal of Civil Engineering*, 27, 949-959.

Hamad, A. J., (2017). "Size and shape effect of specimen on the compressive strength of HPLWFC reinforced with glass fibres." *Journal of King Saud University – Engineering Sciences*, 29, 373-380.

Han, J. W., Lee, S. K., Jeon, J. H., Yu, C., Oh, R. O. and Park, C. G., (2015). "Strength and durability of latex-modified jute/macro-synthetic hybrid fibre-reinforced concrete." *Materials Research Innovations*, 19(5), S5-894-S5-897.

Han, J-W., Jeon, J-H. and Park, C-G., (2015). "Mechanical and permeability characteristics of latex-modified pre-packed pavement repair concrete as a function of the rapid-set binder content." *Materials*, 8, 6728-6737.

Ion, I., Aguiar, J. B., Angelescu, N. and Stanciu, D., (2013). "Properties of polymer modified concrete in fresh and hardened state." *Advanced Materials Research*, 687, 204-212.

Kim, D-H. and Park, C-G., (2013). "Permeability, abrasion, and impact resistance of latex-modified fiber reinforced concrete for precast concrete pavement applications." *Progress in Rubber, Plastics and Recycling Technology*, 29(4), 239-254.

KS, (2010). "*Standard test method for compressive strength of concrete*." KS F 2405, Korean Standard Association.

KS, (2016). "*Method of test for flexural strength of concrete*." KS F 2408, Korean Standard Association.

KS, (2008a). "*Testing method for resistance of concrete to rapid freezing and thawing*." KS F 2456, Korean Standard Association.

KS, (2008b). "*Determination of the water absorption coefficient of building materials*." KS F 2609, Korean Standard Association.

KS, (2012). "*Polymer modified cement mortar for maintenance in concrete structure*." KS F 4042, Korean Standard Association.

Kuhlmann, L. A., (1985). "Latex modified concrete for the repair and rehabilitation of bridges." *International Journal of Cement Composites and Lightweight Concrete*, 7(4), 241-247.

Lee, B. J. and Kim, Y. Y., (2018). "Durability of latex modified concrete mixed with a shrinkage reducing agent for bridge deck pavement." *International Journal of Concrete Structures and Materials*, 12:23. Available at: <https://doi.org/10.1186/s40069-018-0261-8>.

Lee, S-K., Jeon, M-J., Cha, S-S. and Park, C-G., (2017). "Mechanical and permeability characteristics of latex-modified fiber-reinforced roller-compacted rapid-hardening-cement concrete for pavement repair." *Applied Sciences*, 7(7), 694. Available at: <https://doi.org/10.3390/app7070694>.

Li, G., Zhao, X., Rong, C. and Wang, Z., (2010). "Properties of polymer modified steel fiber-reinforced cement concretes." *Construction and Building Materials*, 24, 1201-1206.

Miloud, B., (2005). "Permeability and porosity characteristics of steel fiber reinforced concrete." *Asian Journal of Civil Engineering*, 6(4), 317-330.

MLIT, (2009). "*Concrete Structure Specification*." Ministry of Land, Infrastructure and Transportation, South Korea.

Muhammad, B. and Ismail, M., (2012). "Performance of natural rubber latex modified concrete in acidic and sulfated environments." *Construction and Building Materials*, 31, 129-134.

Nabavi, F., Nejadi, S. and Samali, B., (2013). "Experimental investigation on mix design and mechanical properties of polymer (latex) modified concrete." *Advanced Materials Research*, 687, 112-117.

Oh, R-O., Kim, D-H. and Park, C-G., (2014). "Durability performance of latex modified nylon fiber reinforced concrete for precast concrete pavement applications." *Indian Journal of Engineering and Materials Sciences*, 21, 49-56.

Popovics, S., (1992). "*Concrete materials: Properties, specifications, and testing*." 2nd ed. William Andrew.

Ramakrishnan, V., Wu, G. Y. and Hosalli G., (1989). "Flexural behavior and toughness of fiber reinforced concretes." *Transportation Research Record 1226*, 69-77.

Soroushian, P. and Tlili, A., (1991). "Latex modification effects on the mechanisms of micro crack propagation in concrete materials." *Transportation Research Board*, 1301, 33-39.

Topcu, I. B. and Atesin, O., (2016). "Effect of high dosage lignosulphonate and naphthalene sulphonate based plasticizer usage on micro concrete properties." *Construction and Building Materials*, 120, 189-197.

Wang, M., Wang, R., Zheng, S., Farhan, S., Yao, H. and Jiang, H., (2015). "Research on the chemical mechanism in the polyacrylate latex modified cement system." *Cement and Concrete Research*, 76, 62-69.

Wang, R., Li, X. G. and Wang, P. M., (2006). "Influence of polymer on cement hydration in SBR-modified cement pastes." *Cement and Concrete Research*, 36, 1744-1751.

Xiao, J., Jiang, D., Sha, A. and Huang, Y., (2017). "Effect of styrene – butadiene rubber latex on the properties of modified porous cement – stabilised aggregate." *Road Materials and Pavement Design*. Available at: <https://doi.org/10.1080/14680629.2017.1337042>.

Xu, F., Zhou, M., Chen, J. and Ruan, S., (2014). "Mechanical performance evaluation of polyester fiber and SBR latex compound-modified cement concrete road overlay material." *Construction and Building Materials*, 63, 142-149.

Yang, H., He, Z., Shao, Y. and Li, L., (2018). "Improving freeze-thaw resistance and strength gain of roller compacted fly ash concretes with modified absorbent polymer." *Journal of Materials in Civil Engineering*, 30(3), 04018010.

Yoon, H., Kim, Y. J., Kim, H. S., Kang, J. W. and Koh, H-M., (2017). "Evaluation of early-age concrete compressive strength with ultrasonic sensors." *Sensors*, 17(8), 1817-1~15.